Trapping of gas bubbles in water at a finite distance below a water-solid interface

V. Esteso,[†] S. Carretero-Palacios,[*,†] P. Thiyam,[‡] H. Míguez,[†] D. F. Parsons,[*,¶] I. Brevik,[§] and M. Boström[*,§]

[†]*Multifunctional Optical Materials Group, Instituto de Ciencia de Materiales de Sevilla (Consejo Superior de Investigaciones Científicas - Universidad de Sevilla), Calle Américo Vespucio 49, 41092 Sevilla, Spain*

[‡]*Theoretical Chemistry, Chemical Center, Lund University, SE-223 62 Lund, Sweden*

[¶]*School of Engineering and IT, Murdoch University, 90 South St, Murdoch, WA 6150, Australia*

[§]*Department of Energy and Process Engineering, Norwegian University of Science and Technology, NO-7491 Trondheim, Norway*

E-mail: sol.carretero@csic.es; d.parsons@murdoch.edu.au; mathias.a.bostrom@ntnu.no

Abstract

Gas bubbles in a water filled cavity move upwards due to buoyancy. Near the roof, additional forces come into play, such as Lifshitz, double layer, and hydrodynamic forces. Below uncharged metallic surfaces, repulsive Lifshitz forces combined with buoyancy forces provide a way to trap micrometer sized bubbles. We demonstrate how bubbles of this size can be stably trapped at experimentally accessible distances; the distances being tunable with the surface material. By contrast, large bubbles ($\geq$ 100 μm) are usually pushed towards the roof by buoyancy forces and adhere to the surface. Gas bubbles with radii ranging from 1 to 10 μm can be trapped at equilibrium

distances from 190 nm to 35 nm. As a model for rock, sand grains, and biosurfaces we consider dielectric materials such as silica and polystyrene, whereas aluminium, gold and silver, are examples of metal surfaces. Finally, we demonstrate that a presence of surface charges further strengthens the trapping by inducing ion adsorption forces.

February 26, 2019

Introduction

Gas bubbles can be generated and/or released in water under a variety of situations, from swampy conditions (in which methane, H_2S, or H_2 are released) to ice and gas clathrate (in melting permafrost), biogas (gases produced by the breakdown of organic matter), or biological systems (like aquatic organisms and plants), amongst others. Also, trapped gas bubbles in polar ice cores contain details of the past concentrations of stable atmospheric gases. After water vapor and carbon dioxide, methane and nitrous oxide are the most important long-lived greenhouse gases in the atmosphere. Methane and carbon dioxide concentrations have been frequently measured in polar ice for many years. There is evidence for concluding that the increase in atmospheric greenhouse gas concentrations is well above the range of natural variability for a period over the last 800.000 years .[1,2] Release of trapped greenhouse gas bubbles from melting ice in the arctic due to rising temperatures could substantially enhance climate greenhouse effects and pose hazards to wildlife.

In this work we present a theoretical study on the trapping of released gas bubbles in water below a water-solid interface due to the balance of Lifshitz (f_L) and buoyancy (f_b) forces, as illustrated in Figure 1. A gas bubble of radius R rests at an equilibrium distance d_{eq} from the water-solid top surface as a result of force balance acting on the bubble. To test the generality of our results we study metallic and dielectric surfaces. Besides aluminium (Al), gold (Au) and silver (Ag) metals, well-known metals for which more intense f_L forces are expected, thus with potential nanotechnological applications and for laboratory experimental

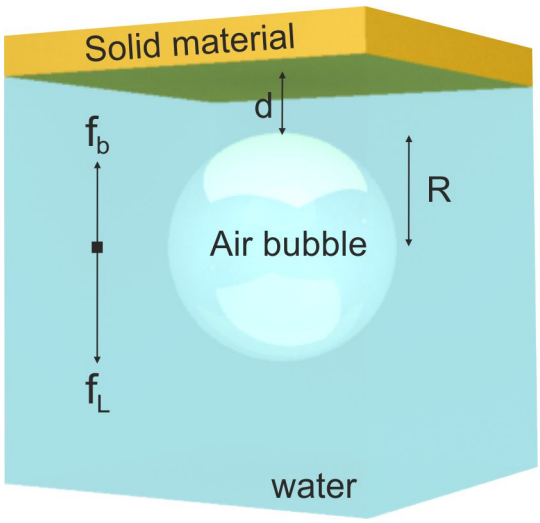

Figure 1: Scheme of the sphere-plane geometry here studied (not to scale). R stands for the radius of the air bubble in pure ice cold water and d is the separation distance between the bubble and the water-solid interface. Here it is considered that $R \gg d$, so that the Derjaguin approximation can be applied. Included in this figure is the Lifshitz force (f_L) and the buoyancy (f_b). We consider also the double layer force (f_{el}) which adds further repulsion to the system.

verification, also two non-metallic surfaces: silica (SiO_2) as model for rock and sand grains, and polystyrene (PS) as a model for biosurfaces. To exemplify the key aspects, we focus on the case when the cavity has uncharged metallic surfaces.

Whereas large gas bubbles ($\gg$ 10 μm) can be mechanically trapped as buoyance is stronger than the repulsive Lifshitz force, or they can be trapped through capillary forces,[3] in this work we focus on the relation between electric and buoyancy forces. Also, we will leave out the hydrodynamic effect of a gas bubble rising with constant velocity u in water far below the planar surface on top. This and other limitations of the model here presented are detailed in section Robustness and Limitations . As the bubble approaches the water-solid surface the velocity goes to zero, with a hydrodynamic force acting on the bubble due to the drainage of water from the film between bubble and solid surface. We may assume that the Reynolds number is small (less than unity), so that the Stokes formula for the drag force, $F = 6\pi\eta u R$, is negligible (here $\eta = 10^{-3}$ Pa·s is the water viscosity). Close to the water-solid interface, the bubble is exposed, amongst others, to a dispersion force which can be described in terms

of the conventional Hamaker constant when the separation distance is very small, $d \leq 10$ nm, or as the full Lifshitz force for larger separations, when electromagnetic retardation effects due to the finite speed of light must be considered. The experiment of Tabor *et al.*[4] is important in this respect, as they investigated the van der Waals interaction between a gas bubble and flat gold, silica, and mica surfaces at distances at which electromagnetic retardation effects do not play a role, i.e., $d \leq 10$ nm. The separation distance between the sphere and the flat surface was found to be the largest for gold (about 10 nm), while for silica that distance was somewhat lower (about 6 nm). These experimental results are in good agreement with theoretical predictions.[5,6] Here, we do not restrict our studies to any separation distance and include electromagnetic retardation effects to analyze an equilibrium situation in which a gas bubble rests near a water-solid surface as a result of the balance of forces acting on it. The Lifshitz (van der Waals) forces that are at play in a system like the one here proposed, can be either attractive or repulsive as was known already to the pioneers .[7] This has been demonstrated many times both theoretically [8–17] and experimentally [4,18–25] in a variety of schemes. What is more fascinating is the fact that equilibrium between repulsive (downward) Lifshitz forces and attractive (upward) buoyancy might cause stable trapping of gas bubbles under water-solid interfaces at distances easily accessible experimentally. We find that equilibrium distances decrease with increasing bubble size, and that trapping is at play for bubbles of micrometer size and smaller. Besides, significant different d_{eq} values are attained for dielectrics and metals. In addition, taking a rock surface or a bed of sand grains (silica) as a representative case, we demonstrate that the presence of surface charge can act to further strengthen the trapping of gas bubbles by inducing ionic adsorption (an electric double layer). Finally, it also turns out that Lifshitz force and buoyancy are more generally dominant at high salt concentrations (> 0.1 M, e.g. in biology, or salt water in the ocean), where charge effects are screened, or at pH values close to the isoelectric point where the water-solid interface is uncharged .[17]

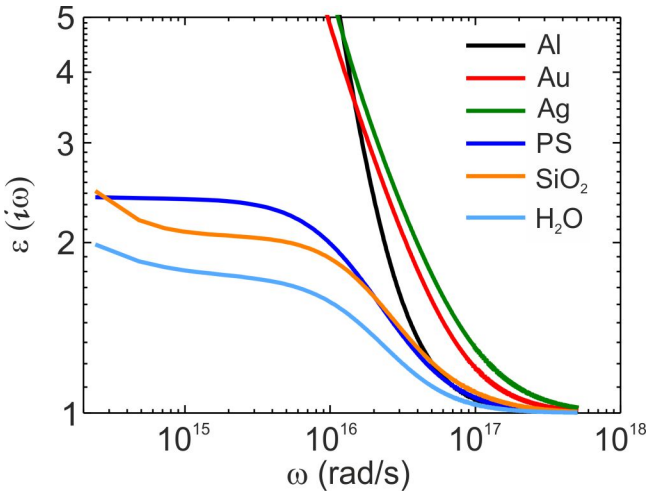

Figure 2: Dielectric function evaluated at the Matsubara frequencies for different materials: Aluminium (black), gold (red), silver (green), polystyrene (dark blue), silica (orange), and water (light blue).

Theory

Consider a gas bubble at equilibrium in pure ice cold water below an uncharged water-solid interface. As mentioned, there are two dominant contributions to the interaction between gas bubble and interface, viz. Lifshitz and buoyancy forces. This model enables us to present the major result which can thereafter be extended if charged surfaces with salt are present. The large gas bubble of radius R has dielectric function ε_1, and is immersed in ice cold water (with ε_2) near a water-solid top surface (with ε_3) at a distance d (see schematics in Figure 1). The size of the bubble fulfills the condition $R \gg d$, so we can use the Derjaguin approximation for the Lifshitz force.[26–28] The Lifshitz force at temperature T can be expressed as a summation of terms taken at Matsubara frequencies ($i\omega_n = i2\pi n k_B T/(\hbar)$, where k_B and $\hbar$ are Boltzmann's, and the reduced Planck's constants, respectively, with $n = 0, 1, 2, ...$):[7,29]

$$f = f_b + f_L = \frac{4\pi R^3}{3} g\Delta\rho + 2\pi R \times k_B T \sum_{n=0}^{\infty}{}' g\left(\omega_n\right). \tag{1}$$

In the above expression, $\Delta\rho$ in the buoyancy term accounts for the density difference between gas ($\rho_g^{T_0} = 1.29$ kg/m^3) and water ($\rho_w^{T_0} = 999.8$ kg/m^3) at $T = 273.15$ K $= 0$°C. In

our calculations we will neglect the slight variation in density (≈ 0.07 %) when temperature changes from $T = 0°$C to $T = 20°$C ($\rho_g^{T20} = 1.20$ kg/m^3 and $\rho_w^{T20} = 999.0$ kg/m^3). Also, in f_L, the prime in the summation of the $n = 0$ Lifshitz term means multiplication by 1/2. In the retarded treatment for the Lifshitz term, there are contributions from transverse magnetic (TM) and transverse electric (TE), $g(\omega_n) = g^{TM}(\omega_n) + g^{TE}(\omega_n)$, where

$$\begin{aligned} g^{TM}(\omega_n) &= \int_0^\infty \tfrac{dqq}{(2\pi)} \ln\left\{1 - e^{-2\gamma_2 d}\left[\tfrac{\varepsilon_1(i\omega_n)\gamma_2 - \varepsilon_2(i\omega_n)\gamma_1}{\varepsilon_1(i\omega_n)\gamma_2 + \varepsilon_2(i\omega_n)\gamma_1}\right]\right. \\ &\qquad \left. \times \left[\tfrac{\varepsilon_3(i\omega_n)\gamma_2 - \varepsilon_2(i\omega_n)\gamma_3}{\varepsilon_3(i\omega_n)\gamma_2 + \varepsilon_2(i\omega_n)\gamma_3}\right]\right\}; \\ g^{TE}(\omega_n) &= \int_0^\infty \tfrac{dqq}{(2\pi)} \ln\left\{1 - e^{-2\gamma_2 d}\left[\tfrac{\gamma_2 - \gamma_1}{\gamma_2 + \gamma_1}\right]\left[\tfrac{\gamma_2 - \gamma_3}{\gamma_2 + \gamma_3}\right]\right\}; \\ \gamma_i &= \sqrt{q^2 - \varepsilon_i(i\omega_n)(i\omega_n/c)^2}. \end{aligned} \tag{2}$$

Here, q stands for the perpendicular wave vector and $\varepsilon_i(i\omega_n) = 1 + 2/\pi \cdot \int_0^\infty \omega \cdot \varepsilon_i''(\omega)/(\omega^2 + i\omega_n^2) d\omega$ is the dielectric function for material i evaluated at the Matsubara frequencies previously described, which depends upon the imaginary part of the dielectric function for material i evaluated at real frequencies, $\varepsilon_i''(\omega)$. In Figure 2, $\varepsilon_i(i\omega_n)$ is depicted for all materials here considered. Remarkably, the dielectric function of water for a wide range of Matsubara frequencies is lower than that of all the other dielectric and metallic materials, so that the necessary condition for attaining repulsive (positive) Lifshitz force[7] $\varepsilon_3(i\omega_n) > \varepsilon_2(i\omega_n) > \varepsilon_1(i\omega_n)$ is fulfilled for the temperatures here evaluated. The effect of thin oxide layers on the metal surface is considered negligible, since even for aluminium the oxide thickness is less than 4 nm,[30] smaller than the equilibrium distances examined here. Note that positive values of f correspond to repulsive forces between the gas bubble and the solid material. We will define the equilibrium distance at which the gas bubble is trapped near a water-solid surface as the distance at which the total force acting on the gas bubble cancels, i.e., $f(d_{eq}) = 0$. Stable trapping will occur only if repulsive forces act at short separation distances and attractive ones at long distances, so that the gas bubble is always pushed back to the equilibrium position if small deviations occur.

In general, surface charges can be set up due to equilibrium of surface groups and ions

present at the interfaces and salt ions in bulk water. We compute ion adsorption forces for a gas bubble near a water-silica interface using a Poisson-Boltzmann description of the aqueous solution at pH 7 (with explicit H^+ and OH^- ions) with NaCl at various concentrations. A charge regulation model[31] was used to determine the surface charge from the pH and the surface potential. We applied Chapel's charge regulation model for the silica surface,[32] a site competition model[33] with an area of 0.5 nm^2 per charge site, and H^+ dissociation constants $pK_H = 6.35$ competing with a metal (Na^+) dissociation constant $pK_M = 3.25$. The total free energy per unit area of the electrolyte between planar surfaces is evaluated from the electrostatic potential and ion concentration profiles[34] and converted to a normalised electrolytic force f_{el}/R using the Derjaguin approximation.

Results

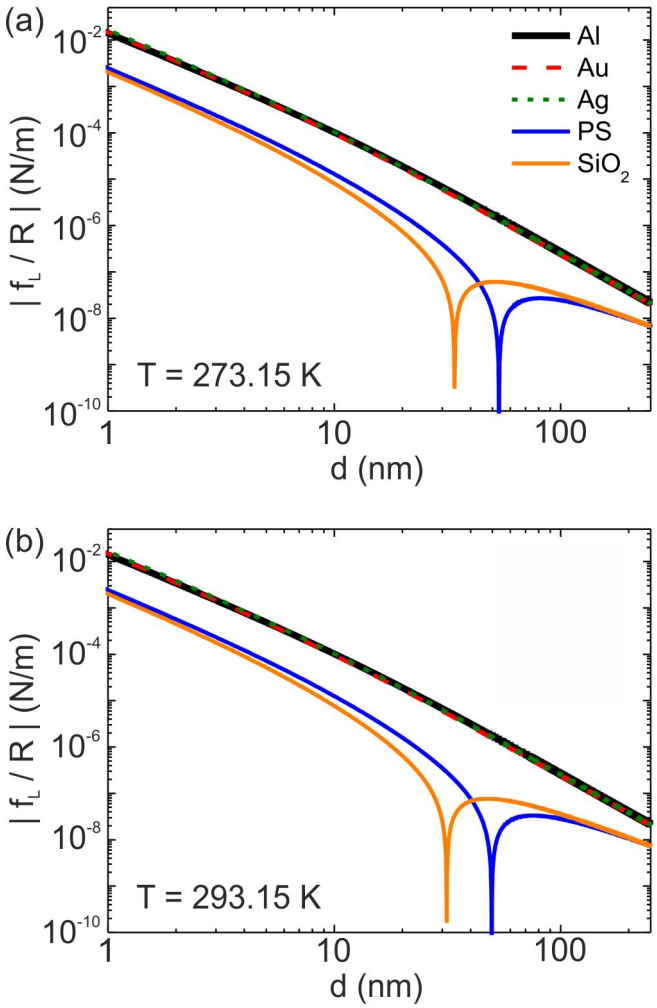

Figure 3: Magnitude of the Lifshitz force per radius as a function of the separation distance for aluminium (black solid line), gold (red dashed line), polysytrene (blue solid line), silver (green short dashed line) and silica (orange solid line), at temperature (a) $T = 0°$C and (b) $T = 20°$C . Forces for metal surfaces are repulsive at all distances, while forces for PS and SiO_2 they are attractive at large distances (> 50 nm).

Figure 3 shows in logarithmic scale the magnitude of the Lifshitz force normalized to the bubble radius ($|f_L/R|$) as a function of the separation distance between a bubble immersed in water and a solid surface. Different dielectric and metallic materials at (a) $T = 0\ ^o$ C and (b) $T = 20\ ^o$ C are investigated. We find that the intensity of f_L/R is larger for metals than for dielectrics, as expected, and whereas metallic surfaces yield repulsive forces at all separation distances, dielectric ones display a change of the force nature from repulsive to

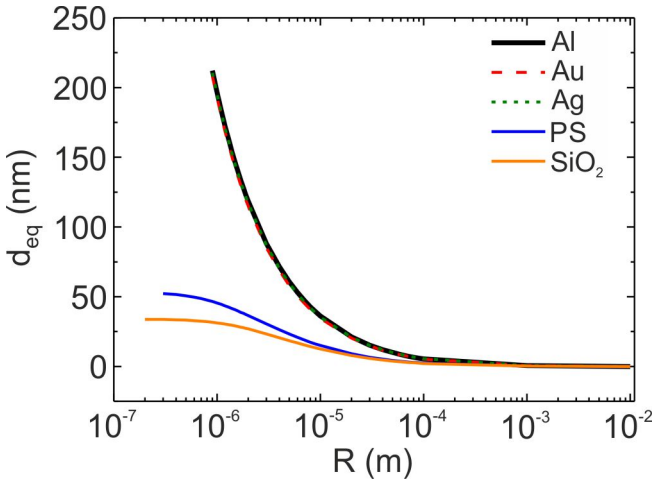

Figure 4: Equilibrium distance as a function of the bubble radius at which the gas bubble gets trapped in pure ice cold water near a water-solid interface at $T = 0°$C being the solid material aluminium (black solid line), gold (red dashed line), polystyrene (blue solid line), silver (green short dashed line) or silica (orange solid line).

attractive as the separation distance between the bubble and the surface increases. Such a change, distinguishable as a sharp minimum in the graph, occurs at different distances for each dielectric material, being larger for PS surfaces. This is due to the dominant term $n = 0$ in the frequency summation, which is negative and intense enough to balance the repulsive contributions when the separation distance is sufficiently large. The negative contribution at $n = 0$ is only given for dielectrics since the static permittivity of water $\varepsilon(0) = 88.2$ is higher than the values for SiO_2 ($\varepsilon(0) = 4$) and PS ($\varepsilon(0) = 2.45$),[12] so that the condition for repulsive force is not fulfilled.[7,24] As the static permittivity of metals tends to infinity, the condition is fulfilled and the term $n = 0$ remains positive (repulsive). In addition, regardless of the specific metallic surface, f_L/R is largely insensitive to the specific metal, making the choice of the metal surface commutable. Finally, we also find that f_L/R hardly varies with a change of temperature for metallic surfaces, whereas slight deviations are encountered for dielectric materials. This slight deviation, quantified as a maximum variation of 9%, hardly affects the equilibrium distance at which gas bubbles are stably trapped.

Figure 4 displays the equilibrium distance as a function of the bubble radius at $T = 0$ ^{o}C for all water-solid materials previously considered. In all cases, the equilibrium distance

decreases with the size of the bubble. This means that for all water-solid interfaces bubbles of size $R \geq 100$ μm will be dominated by buoyancy forces, rising up to the top surface. For smaller bubbles, the trapping distance is larger for metal surfaces (around a few hundred nm) than for dielectric ones (approximately 50 nm), since according to Figure 3, f_L/R is more intense for metallic materials. As expected from results attained in Figure 3, the trapping distance does not depend on the metal surface selected, as f_L/R is found to be almost the same for Au, Ag, and Al surfaces. On the contrary, there are significant changes in the equilibrium distances at which gas bubbles are trapped when dielectric interfaces are involved, being larger for PS surfaces than for SiO_2 ones reflecting the fact that the magnitude of the dielectric function is larger for PS in a large frequency region. Those variations are especially noticeable for smaller bubbles. Besides, the minor variations attained in f_L when temperature varies from $T = 0$ ^{o}C to $T = 20$ ^{o}C (as seen in Figure 3), give rise to maximum changes of around 8 % in the trapping distance near dielectric surfaces, demonstrating the robustness of our results for experimental verification under temperature changes and for exchangeable metallic surfaces.

Finally, Figure 5 shows the sum of ionic double layer force, f_{el} and Lifshitz forces per radius for gas bubbles near a water-solid interface at pH 7 at (a) $T = 0$ °C and (b) $T = 20$ °C. As we mentioned earlier, double layer force can be neglected for biological systems and high salt concentrations (> 0.1M). To exemplify our findings, results are shown for a model system of rock surfaces (i.e. solid silica walls) which possess surface charge. We find that, at low salt concentrations f_{el} adds further repulsion inducing enhanced trapping of gas bubbles. The ionic double layer force is strong for pure water with 10^{-7} M salt concentration. As the salt concentration is increased (> 0.1 M), Lifshitz force and buoyancy dominate and the double layer force will be screened by ions in solution.[17] Again, variations in temperature from $T = 0$ °C to $T = 20$ °C give rise to minor variations in $|(f_L + f_{el})|/R$.

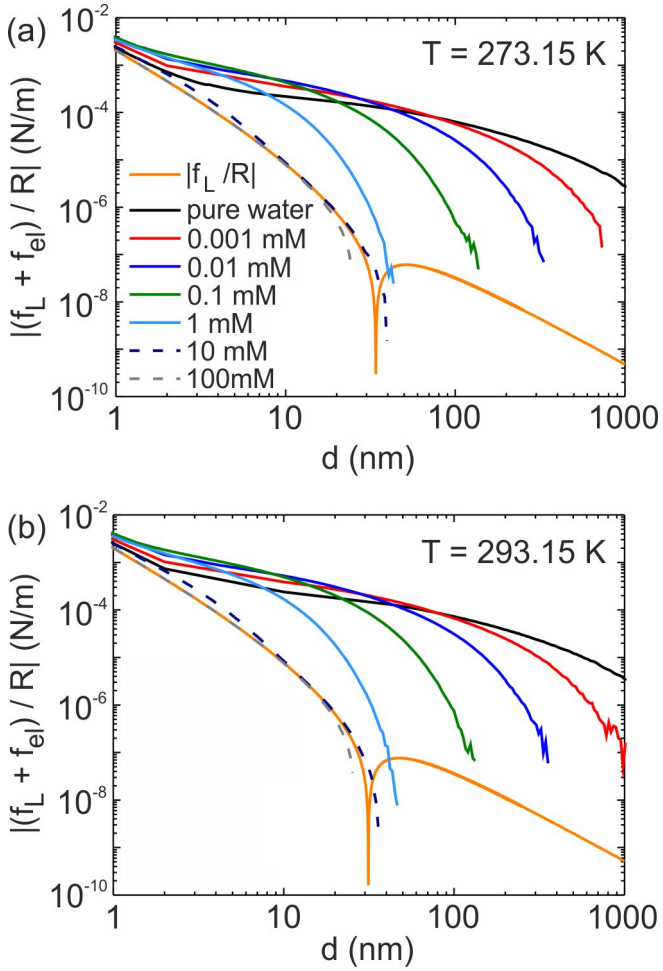

Figure 5: Sum of Lifshitz and double layer force per radius of a gas bubble near a water-silica interface at pH 7 and at temperature (a) $T = 0°C$ and (b) $T = 20°C$ for different salt concentrations (including pure water with a salt concentration of 10^{-7} M). As comparision we also show with only Lifshitz force per radius which agrees with the sum of the two forces around 10-100 mM salt concentration and higher.

Robustness and Limitations

Robustness

We have analyzed the effect of thin solid films (of thicknesses as thin as 40 nm) in comparison to bulk solid materials. As an illustrative case, we consider bubbles of $R = 10\mu$m near an Al or PS surfaces. Figure 6 displays the equilibrium distance as a function of the thickness for both materials. We find, for thin films, maximum deviations (with respect to the bulk material) of $\approx 3\%$ in the trapping distance, demonstrating the power of our findings under

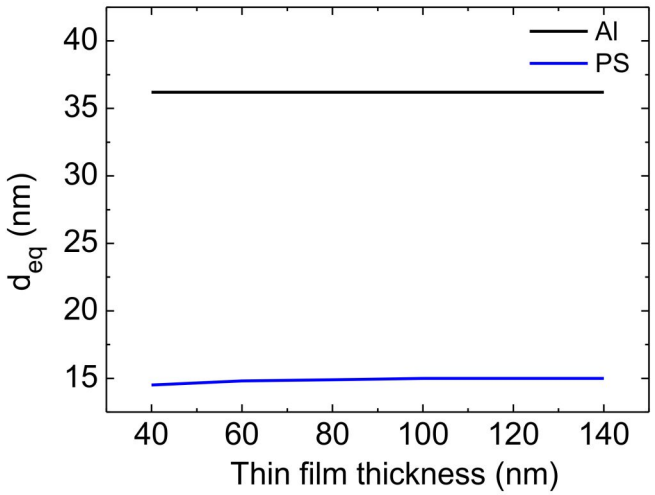

Figure 6: Equilibrium distance at which a gas bubble of $R = 10\mu$m in water at $T = 0°$C gets trapped near a top solid layer, as a function of the thickness of the solid material layer. Calculations for aluminium are shown with a black solid line, and for polystyrene with a blue solid line. Results show that the trapped distance is the same irrespective of the layer thickness of the top surface.

thickness variations.

Limitations

Our treatment above was based upon a simplified model. The behavior of gas bubbles in water is of course a many-facetted phenomenon in general. Let us briefly consider three additional effects that may come into play here.

1) As first point, we mention the effect of gas dissolution. The rate of dm/dt transferred from the interior to the ambient water can in general be analyzed by use of the Ranz-Marshall equation[35]

$$\frac{dm}{dt} = -4\pi R^2 K(c_s - c_i) \tag{3}$$

(here given in general form), where K is the mass transfer coefficient, c_s the equilibrium concentration of the gas/fluid interface, and c_i the local concentration of the dissolved species in the ambient fluid. Whereas the original Ranz-Marshall equation was used to describe evaporation of liquid drops, it has later been applied to describe dissolution of gas bubbles

in plume models.[36–38] For buoyancy-driven air bubbles rising in water, the gas dissolution can be quite appreciable; cf., for instance, Fig. 7 in.[38] However, again because the bubbles are almost at rest at close distances from the roof, we do not think for physical reasons that this effect should be of importance here.

2) The second modifying factor that we will consider in some detail, is the one of deformability of the bubble. In our treatment above, we simply took the bubble to be a sphere of fixed radius. Of course one may inquire if this is a viable assumption, as the bubble is acted upon by dominant buoyancy and Lifshitz forces, and may deform. Let us look into this effect in some detail: The force f on the sphere is essentially the buoyancy force, so that we can put $f = (4\pi R^3/3)g\rho_w$. Close to the surface the bubble is acted upon by the Lifshitz force, corresponding to a local pressure that we shall call P. This pressure acts over an effective area A, whose magnitude is considerably smaller than the full cross section πR^2 of the sphere. For simplicity we put $A = \alpha\pi R^2$ with α a constant, estimated to be of order 0.1. The effective pressure on the upper part of the sphere becomes thus

$$P = \frac{f}{\alpha\pi R^2} = \frac{4Rg\rho_w}{3\alpha}. \tag{4}$$

Assume now cylindrical coordinates, with the z axis pointing upwards. The deflection ζ of the bubble surface, negative because of the repulsive Lifshitz force, and dependent on r only because of azimuthal symmetry, satisfies the local equilibrium condition

$$\gamma\nabla^2\zeta + P = 0, \tag{5}$$

with γ the surface tension coefficient. The solution is

$$\zeta(r) = -\frac{P}{4T}(R^2 - r^2), \tag{6}$$

where we have assumed for simplicity that $\zeta = 0$ far outside the main deflection, at $r = R$.

The maximum deflection $\zeta_{\max}$ occurs at the centerline $r = 0$. Of main interest for us is the relative displacement

$$\frac{\zeta_{\max}}{R} = -\frac{R^2 g \rho_w}{3\alpha\gamma}. \tag{7}$$

With $R = 10^{-4}$ m as a typical radius, and with $\gamma = 0.073$ N/m, we estimate

$$\frac{\zeta_{\max}}{R} \sim -\left(\frac{5}{\alpha}\right) \times 10^{-4}. \tag{8}$$

Taking $\alpha \sim 0.1$ as mentioned above, we thus get

$$\frac{\zeta_{\max}}{R} \sim -5 \times 10^{-3}, \tag{9}$$

The deflection of the bubble surface is quite negligible in comparison to the bubble radius. This simple estimation supports our model above, about a fixed radius of the sphere. The radius of the sphere itself may vary under the influence of the Laplace pressure with $\Delta P = 2\gamma/R$. But the relative deviation in R again is negligible ($\Delta R/R < 10^{-6}$, for a bubble of radius 10 μm that is displaced a distance of 30 μm). The bubbles are stiff under the conditions studied here.

3) As third point, we mention the possible influence of hydrodynamic forces. The drainage of water can play a role in some cases, especially in the case of larger bubbles. However, as discussed already in the Introduction section, this effect is taken as negligible in the present situation as we are considering microbubbles almost at rest, close to the roof.

Conclusions

In conclusion, in this work we have analyzed gas fluxes coming from diverse sources, such as gas pockets in melting ice, hydrates, biogas or aquatic organisms and plants, in the form of bubbles at rest in a water filled cavity under the influence of Lifshitz and buoyancy forces.

Specifically, gas bubbles with radii ranging from 1 to 10 μm can be stably trapped below the interface at equilibrium distances varying from 190 nm to 35 nm due to an interplay between such forces. Moreover, our results are discussed in terms of robustness and limitations of our models. We find that our results are robust with respect to changes in temperature, thickness of the solid top wall, as well as to changes in pore surface materials (we consider model rock, sand grains, and biosurfaces, as well as different metals). In addition, studies on salt concentration demonstrate that the presence of surface charge further strengthens the trapping of gas bubbles by inducing ionic adsorption (double layer force). Larger gas bubbles will be pushed upwards by buoyancy, which might lead to the possibility of diffusion of gas from the upper pore surface. This could lead to release of gas into the surrounding environment via open cracks or pores in the upper surface.

Acknowledgement

We acknowledge support from the Research Council of Norway (Project 250346) and the Spanish Ministry of Science, Innovation and Universities for funding under grant EXPLORA FIS2017-91018-EXP. S.C.-P. acknowledges for funding through a Juan de la Cierva Incorporación under grant IJCI-2016-28549. The project that gave rise to these results received the support of a fellowship granted to V.E. from âĂİla CaixaâĂİ Foundation (ID 100010434). The fellowship code is LCF/BQ/ES15/10360025. This work was supported by resources provided by the Pawsey Supercomputing Centre with funding from the Australian Government and the Government of Western Australia.

References

(1) Wolff, E.; Spahni, R. Methane and nitrous oxide in the ice core record. *Philosophical Transactions of the Royal Society of London A: Mathematical, Physical and Engineering Sciences* **2007**, *365*, 1775–1792.

(2) Wolff, E. W. Greenhouse gases in the Earth system: a palaeoclimate perspective. *Philosophical Transactions of the Royal Society of London A: Mathematical, Physical and Engineering Sciences* **2011**, *369*, 2133–2147.

(3) Mahabadi, N.; Zheng, X.; Yun, T.; van Paassen, L.; Jang, J. Gas Bubble Migration and Trapping in Porous Media: Pore-Scale Simulation. *Journal of Geophysical Research: Solid Earth* **2018**, *123*, 1060–1071.

(4) Tabor, R. F.; Manica, R.; Chan, D. Y. C.; Grieser, F.; Dagastine, R. R. Repulsive van der Waals Forces in Soft Matter: Why Bubbles Do Not Stick to Walls. *Phys. Rev. Lett.* **2011**, *106*, 064501.

(5) Manica, R.; Connor, J. N.; Dagastine, R. R.; Carnie, S. L.; Horn, R. G.; Chan, D. Y. C. Hydrodynamic forces involving deformable interfaces at nanometer separations. *Physics of Fluids* **2008**, *20*, 032101.

(6) Chan, D. Y. C.; Klaseboer, E.; Manica, R. Film drainage and coalescence between deformable drops and bubbles. *Soft Matter* **2011**, *7*, 2235–2264.

(7) Dzyaloshinskii, I.; Lifshitz, E.; Pitaevskii, L. The general theory of van der Waals forces. *Advances in Physics* **1961**, *10*, 165–209.

(8) Ninham, B.; Parsegian, V. van der Waals Forces: Special Characteristics in Lipid-Water Systems and a General Method of Calculation Based on the Lifshitz Theory. *Biophysical Journal* **1970**, *10*, 646 – 663.

(9) Richmond, P.; Ninham, B. Calculations, using Lifshitz theory, of the height vs. thickness for vertical liquid helium films. *Solid State Communications* **1971**, *9*, 1045 – 1047.

(10) Richmond, P.; Ninham, B.; Ottewill, R. A theoretical study of hydrocarbon adsorption on water surfaces using Lifshitz theory. *Journal of Colloid and Interface Science* **1973**, *45*, 69 – 80.

(11) van Zwol, P. J.; Palasantzas, G.; De Hosson, J. T. M. Influence of dielectric properties on van der Waals/Casimir forces in solid-liquid systems. *Phys. Rev. B* **2009**, *79*, 195428.

(12) van Zwol, P. J.; Palasantzas, G. Repulsive Casimir forces between solid materials with high-refractive-index intervening liquids. *Phys. Rev. A* **2010**, *81*, 062502.

(13) Boström, M.; Dou, M.; Thiyam, P.; Parsons, D. F.; Malyi, O. I.; Persson, C. Increased porosity turns desorption to adsorption for gas bubbles near water-SiO_2 interface. *Phys. Rev. B* **2015**, *91*, 075403.

(14) Esteso, V.; Carretero-Palacios, S.; Miguez, H. Nanolevitation Phenomena in Real Plane-Parallel Systems Due to the Balance between Casimir and Gravity Forces. *The Journal of Physical Chemistry C* **2015**, *119*, 5663–5670.

(15) Esteso, V.; Carretero-Palacios, S.; Miguez, H. Effect of temperature variations on equilibrium distances in levitating parallel dielectric plates interacting through Casimir forces. *Journal of Applied Physics* **2016**, *119*, 144301.

(16) Boström, M.; Dou, M.; Malyi, O. I.; Parashar, P.; Parsons, D. F.; Brevik, I.; Persson, C. Fluid-sensitive nanoscale switching with quantum levitation controlled by α-Sn/β-Sn phase transition. *Phys. Rev. B* **2018**, *97*, 125421.

(17) Thiyam, P.; Fiedler, J.; Buhmann, S. Y.; Persson, C.; Brevik, I.; Boström, M.; Parsons, D. F. Ice Particles Sink below the Water Surface Due to a Balance of Salt, van der Waals, and Buoyancy Forces. *The Journal of Physical Chemistry C* **2018**, *122*, 15311–15317.

(18) Anderson, C. H.; Sabisky, E. S. Phonon Interference in Thin Films of Liquid Helium. *Phys. Rev. Lett.* **1970**, *24*, 1049–1052.

(19) Hauxwell, F.; Ottewill, R. A study of the surface of water by hydrocarbon adsorption. *Journal of Colloid and Interface Science* **1970**, *34*, 473 – 479.

(20) Hutter, J. L.; Bechhoefer, J. Manipulation of van der Waals forces to improve image resolution in atomicâĂŘforce microscopy. *Journal of Applied Physics* **1993**, *73*, 4123–4129.

(21) Milling, A.; Mulvaney, P.; Larson, I. Direct Measurement of Repulsive van der Waals Interactions Using an Atomic Force Microscope. *Journal of Colloid and Interface Science* **1996**, *180*, 460 – 465.

(22) woo Lee, S.; Sigmund, W. M. AFM study of repulsive van der Waals forces between Teflon AFâĎć thin film and silica or alumina. *Colloids and Surfaces A: Physicochemical and Engineering Aspects* **2002**, *204*, 43 – 50.

(23) Feiler, A. A.; Bergström, L.; Rutland, M. W. Superlubricity Using Repulsive van der Waals Forces. *Langmuir* **2008**, *24*, 2274 – 2276.

(24) Munday, J. N.; Capasso, F.; Parsegian, V. A. Measured long-range repulsive CasimirâĂŞLifshitz forces. *Nature* **2009**, *457*, 170 – 173.

(25) Le Cunuder, A.; Petrosyan, A.; Palasantzas, G.; Svetovoy, V.; Ciliberto, S. Measurement of the Casimir force in a gas and in a liquid. *Phys. Rev. B* **2018**, *98*, 201408.

(26) Derjaguin, B. V. Untersuchungen über die Reibung und Adhäsion, IV. *Kolloid Z.* **1934**, *69*, 155.

(27) Derjaguin, B. V.; Abrikosova, I. I.; Lifshitz, E. M. Direct measurement of molecular attraction between solids separated by a narrow gap. *Quart. Rev. Chem. Soc.* **1956**, *10*, 295.

(28) Broer, W.; Palasantzas, G.; Knoester, J.; Svetovoy, V. B. Roughness correction to the Casimir force at short separations: Contact distance and extreme value statistic. *Phys. Rev. B* **2012**, *85*, 155410.

(29) Bordag, M.; Klimchitskaya, G. L.; Mohideen, U.; Mostepanenko, V. M. *Advances in the Casimir Effect*; Oxford Science Publications: Oxford, 2009.

(30) Dumas, P.; Dubarry-Barbe, J.; Ere, D.; Levy, Y.; Corset, J. Growth of Thin Alumina Film on Aluminium At Room Temperature : a Kinetic and Spectroscopic Study By Surface Plasmon Excitation Growth of Thin Alu- Mina Film on Aluminium At Room Temperature : a Kinetic and Spectro- Scopic Study By Surface Plasmon Excitati. *Journal de Physique Colloques* **1983**, *44*, C10–205–C10–208.

(31) Ninham, B. W.; Parsegian, V. A. Electrostatic potential between surfaces bearing ionizable groups in ionic equilibrium with physiologic saline solution. *Journal of Theoretical Biology* **1971**, *31*, 405–428.

(32) Chapel, J.-P. Electrolyte Species Dependent Hydration Forces between Silica Surfaces. *Langmuir* **1994**, *10*, 4237–4243.

(33) Parsons, D. F.; Salis, A. The impact of the competitive adsorption of ions at surface sites on surface free energies and surface forces. *The Journal of Chemical Physics* **2015**, *142*, 134707.

(34) Parsons, D. F.; Ninham, B. W. Nonelectrostatic ionic forces between dissimilar surfaces: A mechanism for colloid separation. *Journal of Physical Chemistry C* **2012**, *116*, 7782–7792.

(35) Ranz, W. E.; W. R. Marshall, J. Evaporation from Drops, Parts I. *Chem. Eng. Prog.* **1952**, *48*, 173.

(36) Wüest, A.; Brooks, N. H.; Imboden, D. M. Bubble plume modeling for lake restoration. *Water Resources Research* **1992**, *28*, 3235–3250.

(37) McGinnis, D. F.; Little, J. C. Predicting diffused-bubble oxygen transfer rate using the discrete-bubble model. *Water Research* **2002**, *36*, 4627 – 4635.

(38) Einarsrud, K. E.; Brevik, I. Kinetic Energy Approach to Dissolving Axisymmetric Multiphase Plumes. *J. Hydraulic Eng.* **2009**, *135*, 1041–1051.

Graphical TOC Entry

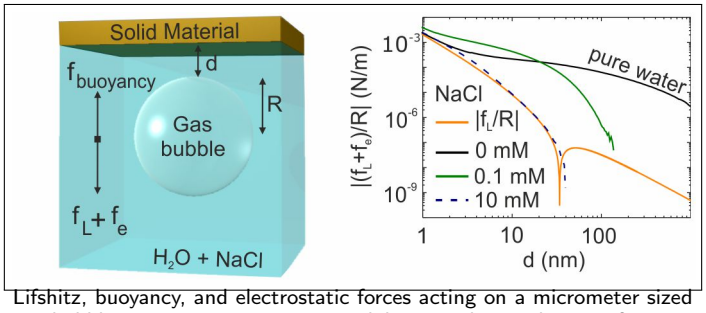

Lifshitz, buoyancy, and electrostatic forces acting on a micrometer sized gas bubble in water near an upper solid material. Results as a function of the distance to the top surface for different salt concentrations are displayed.